7) Coolants for fast neutron Generation IV reactors

Learning outcomes:

After completing this chapter, you will be able to:

1) Design the primary system of a liquid metal cooled reactor to meet constraints for coolant and structural temperatures during nominal operation and design basis accidents;
2) Assess issues related to coolant activation;

Background

As we have seen in the previous chapters of this book, operating a nuclear reactors on a fast neutron spectrum allows achieving the first and second goals of Generation-IV reactors, which can be translated into operating the fuel with a convention ratio larger than unity, in conjunction with the capability of burning minor actinides. The use of liquid metals for transporting the heat produced in the core to a heat sink, and eventually a turbine generator, makes it possible to operate the reactor under ambient pressure, eliminating issues related to loss of pressure accidents. Consequently, all fast neutron power reactors that have been operating were cooled by liquid metals.

The first liquid metal cooled reactor, Clementine, went critical in Los Alamos in 1946 relying on mercury for heat removal. However, it was early on realized that the high vapor pressure of mercury would make the operation of power reactors cooled with mercury difficult. No other elemental metal is liquid at room temperature, but several alloys are, and other metals have melting temperatures low enough to potentially permit their use in a power reactor.

Both sodium and potassium are solid metals at room temperature. At the so-called ”eutectic” composition, consisting of 78 wt% potassium and 22 wt% sodium, corresponding to 68 at% potassium, the melting point of the alloy has a minimum of 260 K. Hence it may be handled without complications of melting and freezing when starting and shutting down the reactor. NaK became the coolant of choice for EBR-I, the Experimental Breeder Reactor in Idaho Falls, which in December 1951 produced the first electricity generated by nuclear power [Marcus 2010]. Beside EBR-I, NaK has been used as coolant in the Dounray Fast Reactor (DFR), as well as for 34 reactors used in space satellites.

Pure sodium was first used as coolant in the SIR/S1G reactor developed by General Electric as a prototype for atomic submarine reactors [GobalSecurity.org]. S1G went critical in May 1955, but operated only for a short time, facing troubles related to sodium leaks. Sodium leaks also caused early shut-down of S2G, deployed in the Seawolf submarine, as well as the Hallam sodium cooled, graphite moderated reactor. A precursor of Hallam known as the Sodium Reactor Experiment (SRE) suffered a partial core melt in 1959. The first reactors to successfully deploy sodium as coolant were BR-5/10 in Russia and EBR-II in the United States, which commenced operation in 1958 and 1963, respectively. Later, Phénix in France became the first industrially sized reactor to operate entirely on plutonium recycled from its own spent fuel, and today BN-600 has produced power to the grid for 40 years with an availability rivaling the best PWRs in Russia. The latest sodium cooled reactor connected to the grid is BN-800, which is intended to function as a fully commercial power plant, operating on mixed oxide fuel. As described in detail in Chapter 1, more than 200 years of operational experience have been accumulated in 25 sodium or NaK-cooled reactors on Earth.

Lead-bismuth eutectic with a composition of 44.5 wt% lead and 55.5 wt% bismuth has a melting temperature of 125°C, and was early on considered as a potential coolant for military sub-marines, both in the United States and the Soviet Union. Whereas the US program was abandoned, the first lead-bismuth cooled reactor, VT-27, was taken into operation in Obninsk in 1959. In spite of observations of corrosion on steam generator tubes in VT-27, the first submarine using reactors this coolant was launched in 1963. Five years later, one of the two K-27 reactors on the K645 submarine suffered a core melt caused by lead-oxide particles blocking a coolant channel. Between 1977 and 1996, six K705 attack submarines operated with oxygen control systems that enabled avoiding problems related to liquid metal corrosion.

The high cost of bismuth, in conjunction with activation under irradiation, makes its use as coolant for commercial reactors less attractive. Pure lead on the other hand has a melting temperature of 327°C, meaning that nominal operating temperatures would be considerably higher than in the submarines, exacerbating thee corrosion issue. To this end, silicon alloyed and aluminium alloyed steels have been developed in Russia and Sweden, respectively, that are believed to be entirely corrosion resistant when exposed to lead up to temperatures of 650-850°C. At the moment of writing, the first power reactor to be cooled by pure lead, BREST-300, is under construction in Russia.

Table 7.1 lists some basic properties of Na, NaK, Pb and PbBi, highlighting the main differences between alkali and heavy liquid metal coolants. Temperature dependent data are given at T = 700 K, and average capture cross sections are given for a representative fast reactor neutron spectrum.

Table 7.1: Properties of alkali and heavy liquid metal coolants

Property	Na	NaK	Pb	PbBi
T_{melt} [K]	371	260	601	399
T_{boil} [K]	1156	1058	2016	1943
ρ [kg/m^3]	850	780	10500	10200
c_p [J/kg/K]	1277	1200	147	144
k [W/m/K]	68	22	17	14
σ_c [mb]	1.3	5.9	4.4	3.6

Liquid metal thermal hydraulics

The thermal hydraulics design of a liquid metal cooled reactor aims at balancing out sometimes conflicting goals, namely:

1) Maximising the thermal power produced by the core;
2) Maximising the efficiency of converting heat to electricity;
3) Ensuring integrity of barriers for fission product release during
   a) nominal operation,
   b) maintenance,
   c) transients;
4) Providing a manageable coolant temperature reactivity feedback.

Goal (4) has been discussed in chapter 2. In order to assess the ability of a design to achieve goal (3), we need to understand aspects of corrosion damage, as well as mechanical strength of materials as function of both temperature and irradiation dose. The latter is discussed in the following chapter, which will be referred to when here needed. In all cases, we must be able to predict temperatures, mass flows, velocity fields and pressure drops under nominal and transient conditions. This is the topic of the current chapter.

The rise in temperature between the inlet and the outlet of the core producing power $\dot{Q}$, is readily obtained from the following relation:

$$\Delta T = \frac{\dot{Q}}{\dot{m}\, c_P},$$

where $\dot{m}$ is the liquid metal mass flow rate through the core and c_P is the specific heat capacity. Thus, increasing the power of the core means increasing ΔT, all other parameters kept constant. In order to compare the heat removal performance of sodium and lead, we may rewrite the mass flow as

$$\dot{m} = \rho v A_{flow}$$

where v is the velocity and A_{flow} is the flow area of the coolant. Figure 7.1 displays the product of density and specific heat capacity, that is the volumetric heat capacity, of sodium and lead as function of temperature.

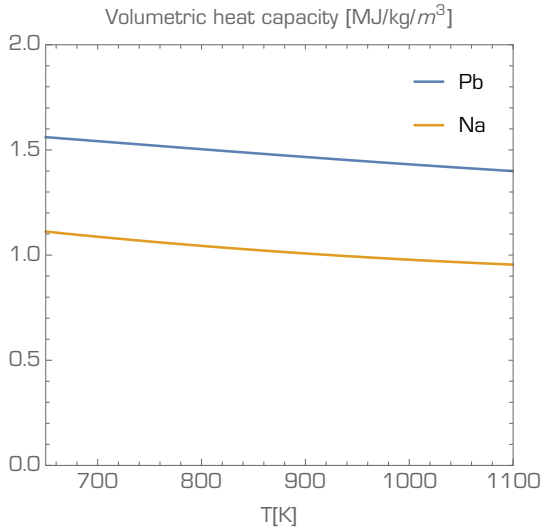

Figure 7.1: Volumetric heat capacity of sodium and lead.

It may be inferred that for a given core power, identical flow areas and velocities, the increase in coolant temperature is larger in sodium than in lead. In practice, the flow velocity in a sodium-cooled reactor is limited to about 8 m/s by the need to avoid mechanical vibrations of fuel rod assemblies [Waltar 1981], whereas in a lead-cooled reactor, it limited to about 2 m/s by other factors, such as erosion, pressure drop and pumping power. Hence, in order to retain a similar temperature difference between inlet and outlet of the core, a the flow area in a lead-cooled reactor has to be about three times larger than in a sodium-cooled reactor. As we have seen in Chapter 2, this has a direct impact on the achievable conversion ratio, which typically will be lower in an LFR than in an SFR having the same fuel composition.

Core temperature profile

Liquid metal cooled reactors traditionally employ hexagonal fuel channel geometry, as illustrated in Figure 7.2, permitting closer packing and smaller neutron leakage.

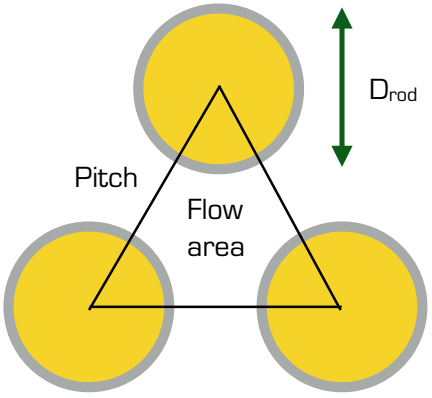

Figure 7.2: Hexagonal fuel channel geometry.

Each fuel channel therefore removes half the pin power, and we may write for the coolant temperature at elevation z:

$$T(z) = T_{in} + \frac{1}{2\dot{m}} \int_{-L/2}^{z} \frac{\chi(z)}{c_p(z)} dz,$$

where L is the fuel column height, the core mid-plane is located at $z = 0$ and $\chi(z)$ is the linear power density of the fuel. In a fast reactor, the latter may be approximated by a cosine distribution:

$$\chi(z) = \chi_{max} \cos\left(\frac{\pi z}{L_0}\right),$$

Where L_0 is the so called "zero flux extrapolation length" illustrated in Figure 7.3.

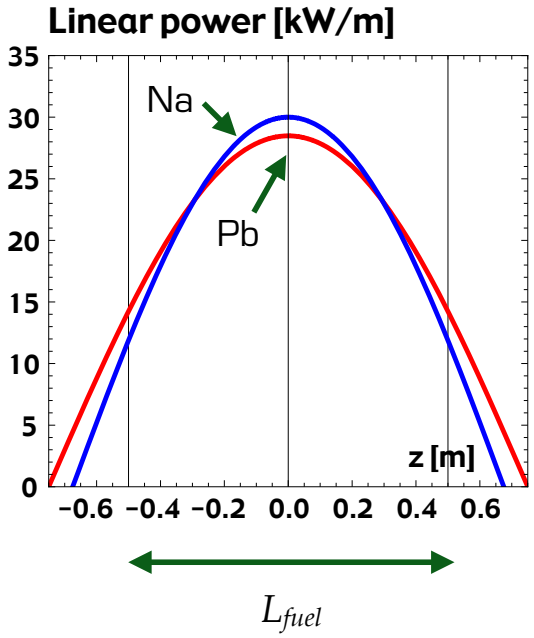

Figure 7.3: Approximate power density profiles in sodium- and lead-cooled reactors.

In a sodium-cooled reactor without axial breeding blankets, the extrapolation length is often found to be 135% of the fuel column height. In lead-cooled reactors, more neutrons are reflected back into the core, resulting in an extrapolation length of about $1.50 \times L$. The average linear power may be found by integrating from bottom to top of the active zone:

$$\chi_{ave} = \frac{1}{L} \int_{-L/2}^{L/2} \chi_{max} \cos\left(\frac{\pi z}{L_0}\right) dz = \frac{2L_0}{\pi L} \chi_{max} \sin\left(\frac{\pi L}{2L_0}\right),$$

which gives the axial power peaking factor:

$$\frac{\chi_{max}}{\chi_{ave}} = \frac{\pi L}{2L_0} \frac{1}{\sin\left(\frac{\pi L}{2L_0}\right)}.$$

If we now approximate the specific heat capacity c_p with its value at the inlet of the core, we may integrate $T(z)$ analytically to find:

$$T(z) \simeq T_{in} + \frac{L\chi_{ave}}{4\dot{m}\, c_p(T_{in})}\left(1 + \frac{\sin\left(\frac{\pi z}{L_0}\right)}{\sin\left(\frac{\pi L}{2L_0}\right)}\right),$$

which at the outlet of the core evaluates as

$$T_{out} \simeq T_{in} + \frac{L\chi_{ave}}{2\dot{m}\, c_p(T_{in})} = T_{in} + \frac{\dot{Q}_{rod}}{2\dot{m}\, c_p(T_{in})}.$$

Expressions for sodium and lead density as function of temperature have been recommended by ANL and NEA (in units of kg/m^3) [Finck 1995, Fazio 2015]:

$$\rho_{Na}(T) = 219 + 275.32\left(1 - \frac{T}{2503.7}\right) + 511.58\left(1 - \frac{T}{2503.7}\right)^{1/2}$$

$$\rho_{Pb}(T) = 11441 - 1.2795 \times T.$$

For the specific heat capacity, the following correlations are suggested, in units of J/kg/K [Finck 1995, Fazio 2015]:

$$c_p^{Na}(T) = 1658.2 - 0.8479 \times T + 4.4541 \times 10^{-4} \times T^2 - \frac{2.9926 \times 10^6}{T^2}$$

$$c_p^{Pb}(T) = 176.2 - 4.923 \times 10^{-2} \times T + 1.544 \times 10^{-5} \times T^2 - \frac{1.524 \times 10^6}{T^2}.$$

All temperatures are given in Kelvin.

In order to compare the temperature profiles in sodium and lead-cooled cores, Figure 7.4 shows the coolant temperature as function of z/L, for mass flows yielding $\Delta T = 100$ K in a channel where the rod power is 30 kW and the inlet temperature is $T_{in} = 673$ K (400°C). The corresponding mass flows are 0.117 kg/s of sodium and 1.02 kg/s of lead.

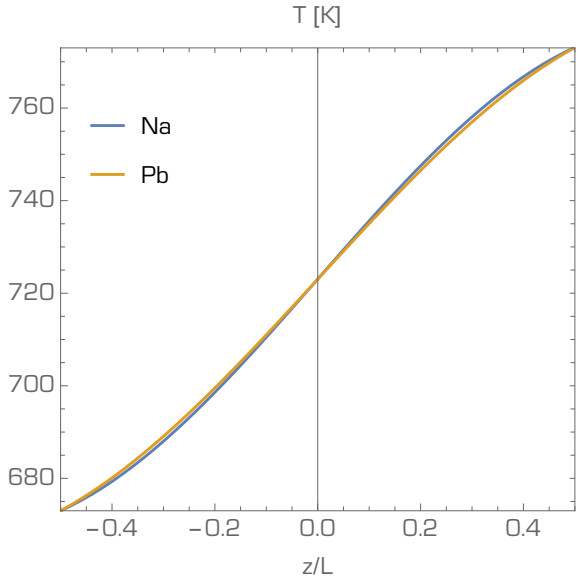

Figure 7.4: Coolant temperature profiles in liquid metal cooled rod lattices where $\Delta T = 100$ for a rod power of 30 kW.

The temperature profiles are very similar in spite of the higher power peaking in the sodium cooled core, and the deviation from a linear dependence is less than 6 K anywhere in the channel.

Heat transfer from fuel cladding to coolant

The heat produced in the fuel pin must be transferred from the cladding tube to the flowing coolant through a boundary layer with laminar or turbulent flow. The heat flux transferred from the cladding to the coolant equals

$$\frac{x(z)}{\pi D_{clad}} = h(T_{out}^{clad} - T_{coolant}).$$

In a simplified treatment, the heat transfer coefficient h can be approximated by

$$h = \frac{Nu \times k}{D_h},$$

Where the hydraulic diameter D_h is the diameter of a tube having the same ratio between tube flow area $A_{tube} = \pi(D_h/2)^2$ and wetted perimeter $P_{wet}^{tube} = \pi D_h$ as the hexagonal rod lattice channel has.

This definition gives us:

$$D_h = \frac{4A_{flow}}{P_{wet}}.$$

In the absence of wire spacers, the wetted perimeter of the hexagonal rod lattice flow channel is (see Figure 7.2):

$$P_{wet} = \frac{1}{2}\pi D_{clad}.$$

Thus, we get for the temperature difference between the cladding and the bulk coolant:

$$T_{out}^{clad} - T_{coolant} = \frac{x(z)}{\pi D_{clad}} \frac{D_h}{Nu \times k},$$

Where the empirically determined Nusselt number Nu is parameterized in terms of the Reynolds and Prandtl numbers. The larger the Nusselt number and the larger the thermal conductivity k of the coolant, the smaller is the temperature drop. The temperature dependence of the thermal conductivity of sodium and lead have been parametrized as [Finck 1995, Fazio 2015]:

$$k_{Na}(T) = 124.67 - 0.11381T + 5.5226 \times 10^{-5}T^2 - 1.1842 \times 10^{-8}T^3$$

$$k_{Pb}(T) = 9.2 + 0.011T.$$

As can bee seen in Figure 7.5, the conductivity of sodium is significantly higher than that of lead.

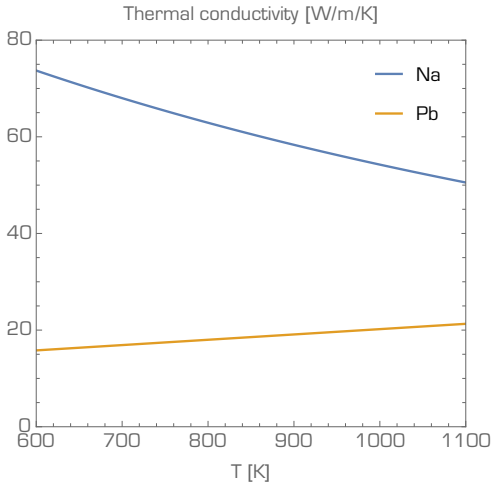

Figure 7.5: Thermal conductivity of sodium and lead as function of temperature.

Based on a careful re-assessment of experimental heat transfer data in liquid metals, Mikityuk found that the following correlation for the Nusselt number best described the available data for hexagonal and square rod lattice channels without spacers [Mikityuk 2009]:

$$Nu = 0.047(1 - e^{-3.8(P/D-1)})(Pe^{0.77} + 250),$$

where P/D is the ratio of the rod pitch and the rod diameter. This correlation is valid for 30 < Pe < 50 000 and 1.10 < P/D < 1.95. The Peclet number Pe is the product of Reynolds and Prandtl numbers:

$$Pe = Re \times Pr,$$

where

$$Re = \frac{\rho v D_h}{\mu} = \frac{\dot{m} D_h}{A_{flow}\mu} = 4\frac{\dot{m}}{P_{wet}\mu}$$

and

$$Pr = \frac{\mu c_p}{k},$$

leading to

$$Pe = \frac{\rho v c_p D_h}{k} = \frac{\dot{m} c_p D_h}{A_{flow} k} = 4\frac{\dot{m} c_p}{P_{wet} k},$$

which is independent of viscosity μ. We may now plot the Nusselt number as function of temperature for the mass flows identified to yield ΔT = 100 K in Figure 7.6. Adopting a sodium velocity of 6.0 m/s and a lead velocity of 1.5 m/s, the corresponding rod pitches are 12.0 mm (Na) and 15.5 mm (Pb). Under these conditions, the Nusselt number of lead is 2.8 times that of sodium at the core inlet temperature of 673 K.

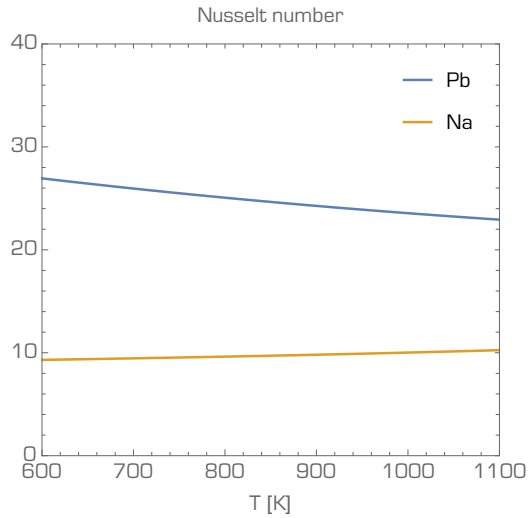

Figure 7.6: Nusselt number of sodium and lead as function of temperature. P/D ratios are 1.20 and 1.55, respectively.

Note that the ratio between thermal conductivity of the two coolants is approximately inverse to the ratio of their Nusselt numbers. Hence, the difference in heat transfer between sodium and lead is mainly determined by the hydraulic diameter of the coolant channel, which is three times larger for the heavy liquid metal. Due to the previously listed limitations to flow velocity, the hydraulic diameter is larger in lead-cooled reactors, resulting in a poorer transfer of heat from the cladding to the bulk coolant. Figure 7.7 shows the resulting temperature drop as function of elevation in the coolant channel where the rod power is 30 kW.

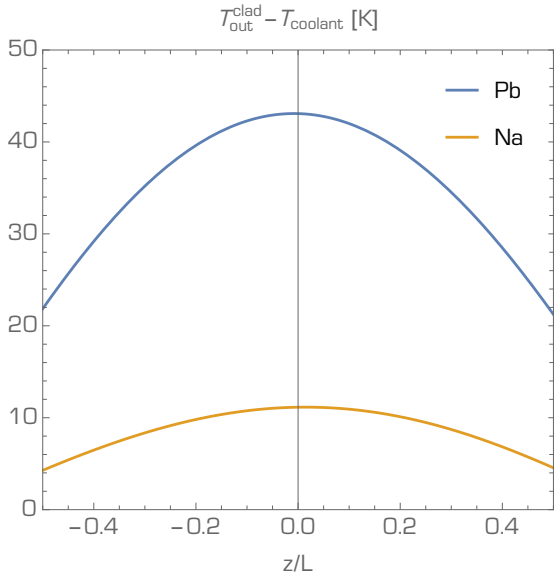

Figure 7.7: ΔT between cladding and bulk coolant in Na and Pb cooled channels, with a rod power of 30 kW, T_{in}^{core} = 673 K, T_{out}^{core} = 773 K and coolant velocities are 6.0 m/s and 1.5 m/s, respectively.

We may finally obtain the cladding temperature in the coolant channel by adding the temperature drop between fuel cladding and bulk coolant to the coolant axial temperature profile illustrated in Figure 7.8. We find that whereas the maximum cladding temperature is observed at the outlet of the sodium-cooled core, the maximum is located slightly below the outlet in the lead-cooled case. For identical coolant inlet/outlet temperatures. The peak cladding surface temperature in the LFR is about 20 K higher than in the SFR.

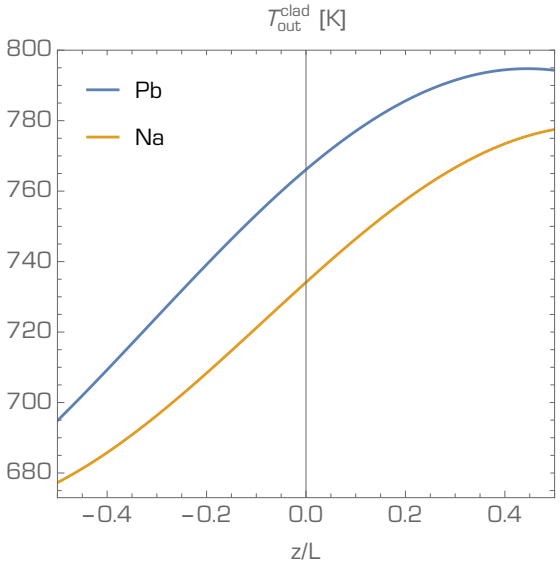

Figure 7.8: Fuel cladding surface temperature in Na and Pb cooled rod channels, where the rod power is 30 kW, T_{in}^{core} = 673 K, T_{out}^{core} = 773 K and coolant velocities are 6.0 m/s and 1.5 m/s, respectively.

Pressure drop

On order to calculate the required pump head during normal operation, and to assess the potential for natural convection for removal of decay heat during transients, we need to predict the pressure drop in the core, the steam generator and other coolant flow paths. A loss of pressure arises when the coolant is accelerated or decelerated. This may occur due to friction in rod bundles, changes in flow area, or a change in flow direction.

The pressure drop in a coolant channel may be written as:

$$\Delta P_{ch} = f \frac{H_{ch} \rho v^2}{2D_h} = f \frac{H_{ch} \dot{m}^2}{2D_h \rho A_{flow}^2}$$

where H_{ch} is the total height of the rod bundle, and f is the channel friction factor. In absence of wire spacers, the friction factor may be approximated by the empirical Blasius correlation:

$$f = \frac{0.316}{Re^{0.25}}.$$

Hence, the dependence on the Reynolds number is relatively weak. In order to evaluate the Reynolds number for the coolant channel flow, we apply the expressions for the dynamic viscosity μ provided by ANL and NEA [Finck 1995, Fazio 2015]:

$$\mu_{Na}(T) = \frac{e^{-6.4406+556.835/T}}{T^{0.3958}}$$

$$\mu_{Pb}(T) = 4.55 \times 10^{-4} e^{1069/T}.$$

Figure 7.9 illustrates the dependence of Reynolds number on temperature, in a coolant channel with rod diameter of 10.0 mm and mass flows yielding ΔT = 100 K for a rod power of 30 kW.

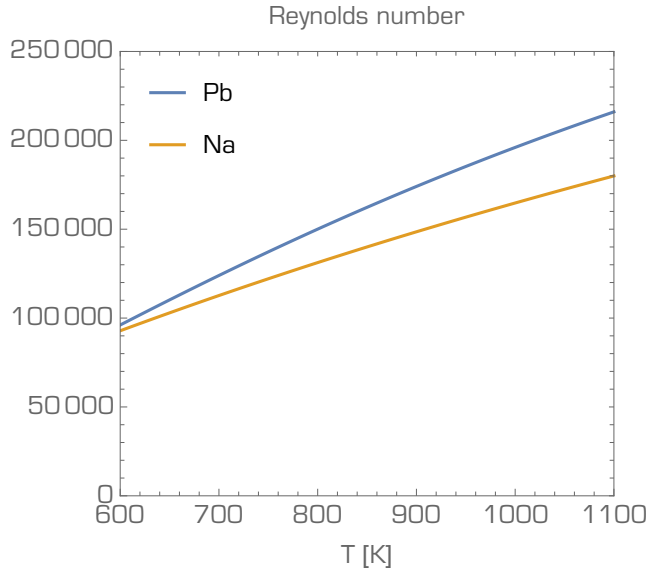

Figure 7.9: Reynolds number in Na and Pb cooled hexagonal flow channels, where the rod power is 30 kW, the rod diameter is 10 mm, $T_{in}^{core} = 673$ K, $T_{out}^{core} = 773$ K and coolant velocities are 6.0 m/s and 1.5 m/s, respectively.

The Reynolds numbers of sodium and lead are of similar magnitude, and increase with temperature. The corresponding channel friction factors are of the order of 0.01-0.02.

We may now compare the magnitude of the the channel friction pressure drop in sodium and lead-cooled cores. Figure 7.10 displays ΔP_{ch} per meter of channel height, as function of normalized coolant velocity, in this case relative to 6.0 m/s for sodium and relative to 1.5 m/s for lead.

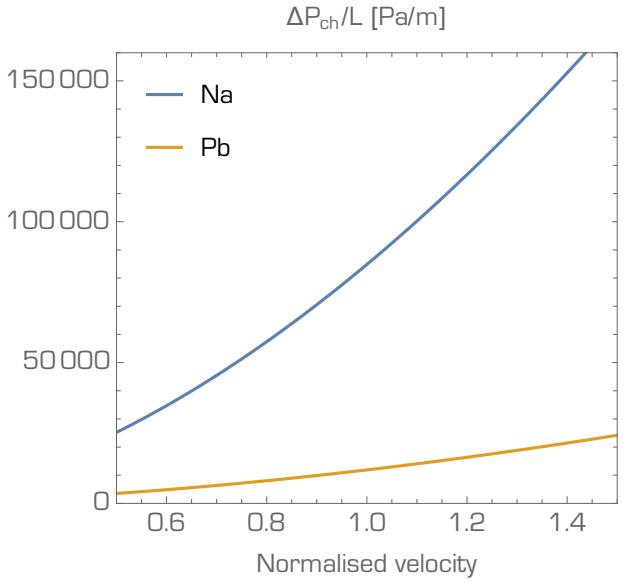

Figure 7.10: Channel friction pressure drop per meter of hexagonal flow channel, where the rod diameter is 10 mm, $T_{in}^{core} = 673$ K, $T_{out}^{core} = 773$ K and velocities are given relative to 6.0 m/s for Na and 1.5 m/s for Pb.

In the SFR, the channel friction pressure drop is a factor seven higher than in the LFR, which mainly is due to the four times higher flow velocity. Reducing the velocity of sodium by a factor of three would yield the same pressure drop as in the lead cooled channel.

In addition to the channel friction pressure drop, there are significant pressure loss related to the sudden change in flow area when the coolant enters and exists the rod bundle. These losses may be written as [Idelchik 1996]:

$$\Delta P_{in} = \frac{1}{2}\left(1 - \frac{A_{flow}}{A_{wrapper}}\right)\frac{\dot{m}^2}{2\rho A_{flow}^2},$$

when entering the bundle, and

$$\Delta P_{out} = \left(1 - \frac{A_{flow}}{A_{wrapper}}\right)^2 \frac{\dot{m}^2}{2\rho A_{flow}^2},$$

when exiting the bundle. For the here studied geometrical configurations these pressure losses sum up to about 11 kPa in the sodium-cooled channel and 4 kPa in the lead-cooled channel.

Relative to the channel friction pressure drop, these play a more significant role in the LFR geometry, since channel friction scales inversely with its hydraulic diameter, which is three times larger for lead. Similar expressions may be defined for pressure drops at the inlet and outlet of the fuel assembly foot and the fuel assembly exit. The magnitudes of these losses are design dependent, but would in general be smaller than the pressure drops related to entering and exiting the rod bundle.

So far, we have ignored the presence of rod spacers. In sodium cooled reactors, these are almost exclusively of wire design, which minimize the impact on the coolant flow. A careful evaluation of experimental data for pressure drops in wire-spaced rod bundles was carried out by Rehme and, and critically reviewed by Bubelis [Rehme 1973, Bubelis 2008]. The correlation suggested by Rehme is relatively complex and out of the scope of the present text-book. Figure 7.11 illustrates the deviation from the channel friction factor f that is suggested by the correlation of Rehme, from which it may be implied that the discrepancy becomes important for Reynolds numbers below 10 000. Hence, it may be neglected for nominal operation conditions, but should be taken into account for transitions to natural convection.

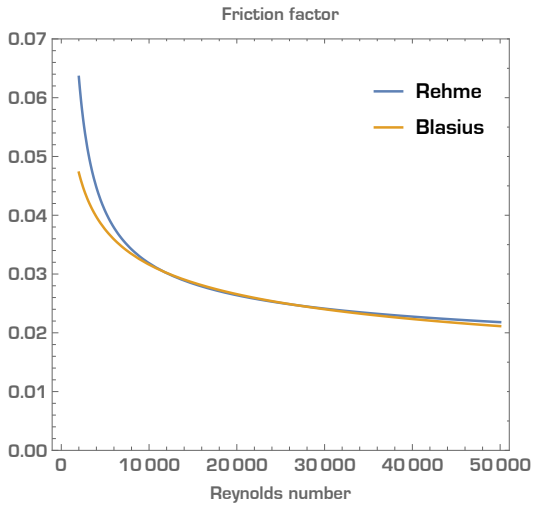

Figure 7.11: Channel friction factor proposed by Rehme for wire spaced rod bundles, compared to the Blasius expression.

In the case of grid spacers, Rehme suggested the following expression for the associated pressure drop over a single spacer [Rehme 1973]:

$$\Delta P_{spacer} = K_{spacer}\left(1 - \frac{A_{spacer}}{A_{flow}}\right)^2 \frac{\dot{m}^2}{2\rho A_{flow}^2},$$

where the grid loss coefficient has to be determined for each particular spacer design. A value of $K_{spacer} \simeq 7.0$ is suggested by experiments conducted by ENEA [Petrazzini 2008]. A well designed grid spacer may occupy 20% of the low area, leading to a pressure loss over a single spacer equal to 3 kPa if applied to the LFR configuration here studied. As a rough guidance, two spacers per meter of coolant

channel may be required.

Forced and natural convection

During nominal operation, the pressure losses, and therefore the pump head in the primary circuit of an SFR is about seven times higher than in the corresponding LFR. The associated hydraulic pumping power is given by:

$$P_{hydraulic} = g\dot{m}P_{head}.$$

Since the mass flow rate in the lead-cooled reactor is nine times higher for the same ΔT over the core, the required pumping power in the LFR is 25% higher than in the SFR.

The associated hydraulic pumping power is 8-10 W for removal of 15 kW fission power dissipated into a single coolant channel. The efficiency in converting electrical power to hydraulic power is 60-85% for a centrifugal pump. In the same time, the efficiency for converting fission power to electricity in a liquid metal cooled reactor is about 40%. Hence, 1.5-3.0 percent of the electrical power produced is consumed by the pumps.

In the case of pump failure, loss-of-flow will result, leading to an initial increase in coolant and fuel temperatures. A well designed Generation IV reactor exhibits negative temperature feedbacks, which will render the core sub-critical. The residual heat consists of a combination of delayed neutron induced fission heating and heating from decay of fission products and short-lived actinides. A passively safe reactor shall be able to remove this heat from the core by natural convection of the primary coolant.

As illustrated in Figure 7.12, the hot coolant above the core has a lower density than the cold coolant at the outlet of the heat exchanger. This will create a buoyancy pressure head P_b having a magnitude

$$P_b = gH_{HX}(\rho_{cold} - \rho_{hot}),$$

Where H_{HX} is the difference in elevation between the thermal centers of the core and the heat exchanger. In the case on an LFR, the heat exchanger would be a steam generator.

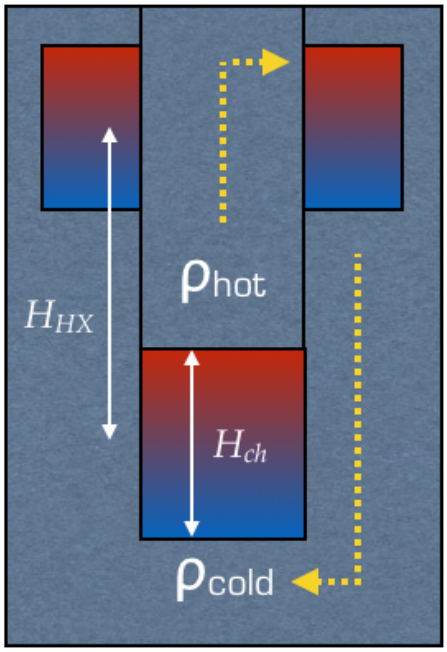

Figure 7.12: The main parameters governing natural convection of liquid metal coolants.

At fully established natural convection, this buoyancy pressure equals the sum of pressure losses in the primary system. Recalling the expressions for liquid metal density as function of temperature we have:

$$\frac{\Delta\rho_{Na}}{\Delta T_{Na}} \simeq 22\ kg/m^3/K$$

$$\frac{\Delta\rho_{Pb}}{\Delta T_{Pb}} \simeq 128\ kg/m^3/K.$$

Hence, for the same temperature gradient, the buoyancy head is about six times larger in an LFR. Multiplying with the gravitational constant, the attainable pressure head is 1.3 kPa per meter of elevation of the steam generator in a lead-cooled reactor.

Now, let us investigate the a situation where the residual heat amounts to 10% of the nominal power of the core. Most of this power would be produced by delayed neutron induced fission. In order to retain the same ΔT over the core, the coolant mass flow rate may decrease to 10% of the nominal value. If we for a moment neglect the dependence of the channel friction factor on Reynolds number (hence mass flow), all pressure drops are proportional to the square of the mass flow rate. One may then infer that the system pressure drop under natural convection conditions should be a factor 100 lower than the nominal value. If the latter is 100 kPa, the required buoyancy head will be 1.0 kPa, which in an LFR is attainable for an elevation of the steam generator thermal centre equal to 0.75 meters. Adjusting for the increase in friction factor when the Reynolds number is of the order of 10 000 rather than 100 000 yields an elevation of about 1.0 m.

If the SFR has a primary circuit pressure drop of 5 bars during nominal operation, the pressure head necessary to remove 10% residual heat with no increase in ΔT would be 5 kPa. Due to the six times smaller specific buoyancy head, the required elevation of the heat exchanger dedicated to residual heat removal (the DHR system) would be of the order of 30 meters!

Hence, a sodium-cooled reactor is difficult to design so that an un-protected loss-of-flow event can be managed in a passive manner. On the other hand, the ability of a lead-cooled reactor to remove residual heat in a very compact format is a significant advantage when considering passive safety performance.

Exercises:

1) Assess the impact of the presence of a wire spacer in a sodium-cooled rod channel. How does it affect the coolant flow area, wetter perimeter and hydraulic diameter? What is the resulting increase in rod pitch that must be applied to retain ΔT = 100 K for a rod power of 30 kW? How is the channel friction pressure drop affected?
2) Assess the impact of the presence of grid spacers in a lead-cooled rod channel. How does it affect the coolant flow area, wetter perimeter and hydraulic diameter? What is the resulting increase in rod pitch that must be applied to retain ΔT = 100 K for a rod power of 30 kW? How is the channel friction pressure drop affected?
3) Use Serpent to calculate the activation of sodium, lead and lead-bismuth coolants.

Questions:

1) Why does sodium perform better as a coolant during nominal operation?
2) What makes lead a better choice for passive decay heat removal?
3) How does coolant activation impact operation, maintenance and decommissioning?

References

E. Bubelis, and M Schikorr,
Review and proposal for best-fit of wire-wrapped fuel bundle friction factor and pressure drop predictions using various existing correlations.
Nuclear Engineering and Design **238** (2008) 3299.

Concetta Fazio, editor,
Handbook on Lead-bismuth Eutectic Alloy and Lead Properties, Materials Compatibility, Thermal-hydraulics and Technologies,
NEA No. 7268, OECD/NEA, 2015.

J. K. Fink and L. Leibowitz,
Thermodynamic and Transport Properties of Sodium Liquid and Vapor,
ANL/RE-95/2, Argonne National Laboratory, 1995.

Global Security,
S1G,
https://www.globalsecurity.org/military/systems/ship/systems/s1g.htm, Downloaded 2020-09-14.

I.E. Idelchik,
Handbook of hydraulic resistance,
Hemisphere publishing corporation, 1996.

Gail H. Marcus,
Nuclear Firsts: Milestones on the Road to Nuclear Power Development,
American Nuclear Society, 2010.

K. Mikityuk,
Heat transfer to liquid metal: review of data and correlations for tube bundles.
Nuclear Engineering and Design **239** (2009) 680.

M. Petrazzini,
Main components functional sizing of EFIT,
EUROTRANS deliverable D1.24, Ansaldo Nucleare 2008.

K. Rehme,
Pressure drop correlations for fuel element spacers.
Nuclear Technology **17** (1973) 15.

Alan E. Waltar and Albert B. Reynolds,
Fast Breeder Reactors.
Pergamon Press, 1981.